Design and Synthesis of Triptycene-containing Polyimide Membranes with Tunable Fractional Free Volume for Gas Separation Applications

Patrick Buckley
Department of Chemical and Biomolecular Engineering
Advisor: Dr. Ruilan Guo

The objective of this research project is to develop new triptycene-containing polyimide membranes with the potential for high performance gas separation. Polymer membrane gas separation capabilities are judged by their combination of permeability and selectivity. Permeability determines how easily the gas molecules pass through the membrane, while the selectivity is a measure of the sieving capabilities of the membrane. Ideally, a membrane would have high selectivity and high permeability, but generally a trade-off exists between these two properties, in which a high permeability results in a low selectivity and vice versa. This project sought to overcome this trade-off by tuning the membrane fractional free volume through the careful design of the polymer backbone structure. Triptycene, a rigid and bulky molecule with high internal free volume, was incorporated into a polyimide backbone structure in order to simultaneously enhance permeability and selectivity. In this project, amine functionality was introduced directly onto the triptycene skeleton to create a highly rigid and contorted backbone structure.

The triptycene diamine monomer was synthesized from benzoquinone and anthracene. The Diels-Alder reaction produced a 1,4-triptycene skeleton, which was first reduced to hydroquinone and then oxidized to conjugated quinone. This product was then converted to a dioxime, which was further reduced to the diamine functionality, the final triptycene monomer. The reaction scheme is shown below. Each step of this monomer synthesis was monitored with

proton nuclear magnetic resonance (^{1}H NMR) spectroscopy to confirm that right chemical structure and high purity was obtained. See below for sample spectra.

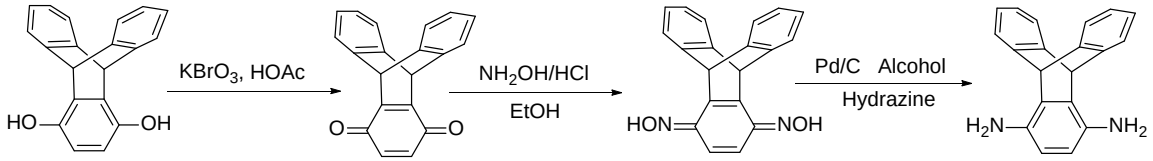

Scheme1. Synthesis of triptycene-1,4-diamine

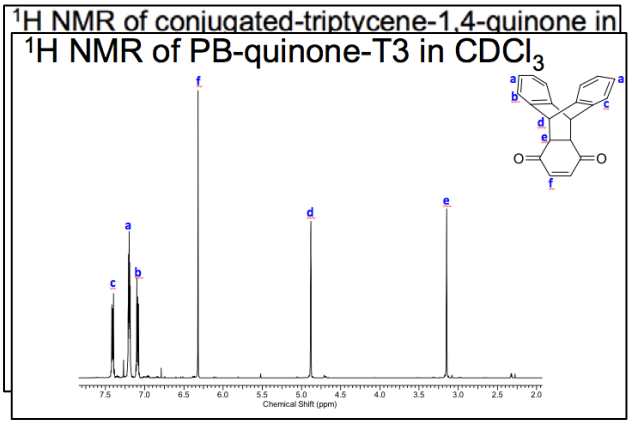

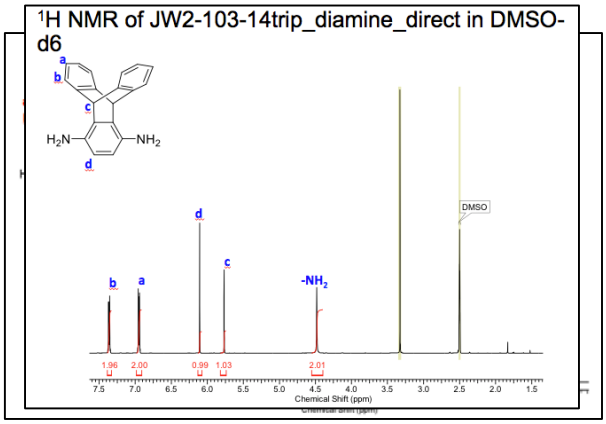

To obtain the triptycene-based polyimide, the diamine monomer was polymerized with commercially available 4,4'-hexafluoroisopropylidine bisphthalic dianhydride (6FDA), as shown below. Several different polymerization methods were attempted to form the polyimide, including chemical imidization, thermal imidization, and an ester-acid method. Membranes were fabricated using the resulting polyimides. To do this, the polymer fibers were dissolved in N-methyl-2-pyrrolidone (NMP), filtered to remove any impurities, and poured onto a leveled glass

plate. Drying overnight under an infrared lamp then formed the film. For all the trials, the membrane film casting was unsuccessful. The membrane cracked into thin strands that would not be serviceable for gas separation. The poor membrane formation was most likely due to a low polymer molecular weight. While no useable films were obtained, proton NMR was used to confirm that the expected polyimide structure was obtained with good purity. Therefore, the next step for this project is to further improve the monomer purity to facilitate condensation polymerization to obtain a higher molecular weight polyimide product.

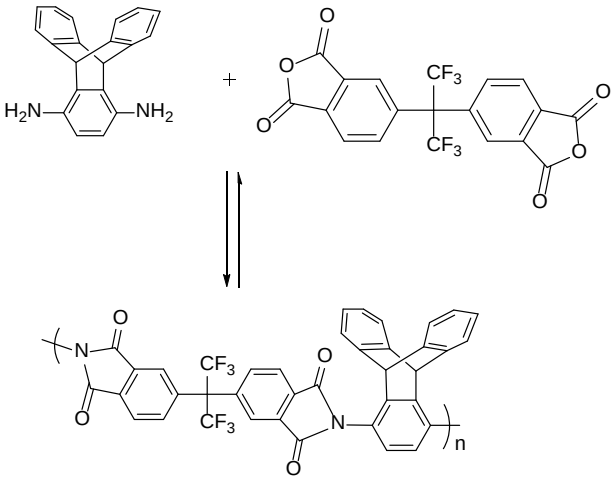

Scheme 2. Synthesis of triptycene-polyimides via condensation polymerization

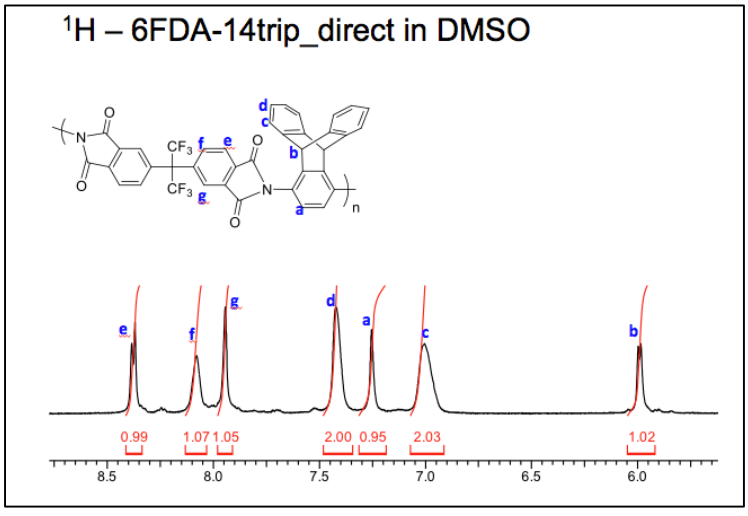

Poster Presentation

Using the Natural Bond Orbitals of Ionic Liquids to Predict Relative CO_2 Binding Strength

Sean Dwyer
Advisors: William Schneider, Dept. of Chemical and Biomolecular Engineering and Chemistry and Biochemistry, and Tae Lee, Dept. of Chemical and Biomolecular Engineering, University of Notre Dame

Ionic liquids can bind selectively and reversible with CO_2. This allows ionic liquids to be an effective and environmentally friendly way to reduce CO_2 emissions. The important chemical properties of ionic liquids that allow for CO_2 capture are caused by its electronic structure. The goal of this research is to better understand the electronic structure of ionic liquids, in order to predict the relative strength of CO_2 capture. To do this, Natural Bond Orbital analysis is used. NBO analysis is an effective computational method which can represent a complicated electronic structure as "Lewis-like" orbitals. This allows for a localized understanding of charge and energy. This research uses the NBO analysis on a one ion pair module of several different ionic liquids, in order to determine the effects that orbital energy and charge have on CO_2 binding. While it was previously reported that an anion only module was unable to predict relative CO_2 binding enthalpy, the ion pair module is able to predict the relative CO_2 binding enthalpy. It was found that the anion's orbital energy and charge depended on the cation, as well as the distance between the cation and anion, further showing the importance of the cation's role in CO2 binding. The orbital energy and charge of the CO_2 reaction site were found to be linearly related to the CO_2 binding enthalpy.

2014 Slatt Fellowship

Matthew Feeley, Department of Physics
Dr. Fabio Semperlotti, Department of Aerospace and Mechanical Engineering

Interaction between Elasticity and Heat Transfer in Thermoacoustic Waves in Multi-Dimensional Solids

Project Description: This mode of heat transfer is largely unexplored, but understanding the interaction between elasticity and heat transfer could realize several energy harvesting technologies that do not exist today. For example, we could develop devices that utilize solid-state refrigeration, control heat transfer by acoustic waves and take non-intrusive temperature measurements in 3D solids. The skeleton of the theory has been derived, and I intend to expand it into multi-dimensions. After acquiring theoretical results, I will quantify these effects via a numerical simulation by investigating them in a solid at a known uniform temperature. My results will provide insight on how to control the heat transfer by thermoacoustic waves. Finally, we will use a simple experiment to apply our theory to a solid-state refrigerator. It is also worth noting that this project will build on the numerical and experimental results that were obtained by another undergraduate researcher supported by Slatt Fellowship 2013.

Project Results: I spent this year designing and testing a "refrigerating shoe". The shoe converts mechanical energy of walking in to thermal energy, of the wearer's comfort. Once the design phase was completed, we proceeded to complete a series of tests on the shoe. The purpose of testing this shoe was to show that the refrigeration effect, which was previously demonstrated on a larger scale, could still work on a smaller scale. I think our results were encouraging. We were able to produce a temperature difference by only utilizing two small chambers (one of which was hardly compressible). However, I think that for a manufacturer to be totally convinced that they should further develop this idea into a product, they are going to want to know the following:

1. How incorporating other chambers will improve the performance of the shoe.
2. How the fluid dynamics within the chambers will be regulated, so that, if a person wants to harness warmth, for example, the warm air can come in contact with his foot.

View Abstract

ABSTRACT SYMPOSIUM NAME: Coordination Chemistry: Characterization and Applications - Poster

ABSTRACT SYMPOSIUM PROGRAM AREA NAME: [INOR] Division of Inorganic Chemistry

CONTROL ID: 2124284

PRESENTATION TYPE: Poster Only : Consider for Sci-Mix

TITLE: Electronic structure and reactivity of d^0 Mo and Ti complexes of a tris-aminophenolate ligand

AUTHORS (FIRST NAME, LAST NAME): Travis Marshall-Roth[1], Seth N. Brown[1]

INSTITUTIONS (ALL): 1. Department of Chemistry and Biochemistry, University of Notre Dame, Notre Dame, IN, United States.

ABSTRACT BODY:

Abstract: Nonclassical redox reactions involve bond formation at a metal center facilitated by oxidation of the surrounding ligands. In order to discourage ligand dissociation upon oxidation, a novel tripodal tris(aminophenol) ligand, tris(4-methyl-2-((3',5'-di-*tert*-butyl-2'-hydroxyphenyl)amino)phenyl)amine, $MeClampH_6$, was prepared. Its diamagnetic molybdenum(VI) complex features a capped octahedral geometry with significant π donation from the three redox-active amidophenolate orbitals. Each amidophenolate displays a calculated metrical oxidation state of about -1.5 and a π bond order of 2/3. Analysis of the optical bands representing the *a* (π_{nb}) → *e* ($d\pi^*$) and *e* (π_b) → *e* ($d\pi^*$) transitions in neutral (MeClamp)Mo gives an estimate of 40 kcal/mol stabilization per π bond. The titanium(IV) analogue (MeClamp)Ti (shown below) is a diamagnetic, unsymmetrical κ^6 complex with a doubly oxidized ligand and weaker π bonding. Evidence of catalytic oxidation of benzylic and aliphatic alcohols to aldehydes under aerobic conditions by (MeClamp)Ti will be presented.

(No Table Selected)

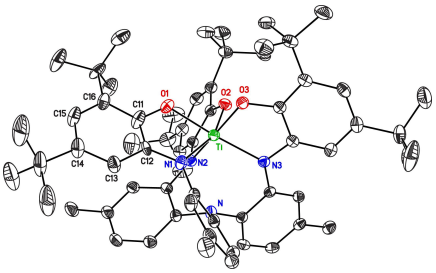

Dalton Transactions

PAPER

View Article Online
View Journal | View Issue

Cite this: *Dalton Trans.*, 2015, **44**, 677

Redox activity and π bonding in a tripodal seven-coordinate molybdenum(VI) tris(amidophenolate)†

Travis Marshall-Roth and Seth N. Brown*

Received 24th September 2014,
Accepted 23rd October 2014

DOI: 10.1039/c4dt02936d

www.rsc.org/dalton

A tris(aminophenol), tris(2-(3′,5′-di-*tert*-butyl-2′-hydroxyphenyl)amino-4-methylphenyl)amine, MeClampH$_6$, is prepared in three steps from tri-*p*-tolylamine. The ligand reacts with dioxomolybdenum(VI) bis(acetylacetonate) to form an oxo-free heptadentate complex, (MeClamp)Mo, with a capped octahedral geometry. The molybdenum is formally in the +6 oxidation state, with significant π donation of the amidophenolates, as judged by intraligand bond distances. Two ligand-based oxidations and one metal-centered reduction are observed by cyclic voltammetry. Analysis of the optical spectrum of the compound gives an estimate of the energetic stabilization of the ligand π orbitals by bonding to the molybdenum of approximately 0.9 eV, corresponding to about 40 kcal mol^{-1} per π bond.

Introduction

Tripodal ligands contain a central donor atom, typically nitrogen or phosphorus, attached to three arms that contain additional donor atoms. These strongly chelating ligands are capable of stabilizing unusual geometries such as trigonal monopyramids,[1] but are also often observed in trigonal bipyramidal or octahedral geometries. They have been used to protect metal centers against hydrolysis,[2] to maintain mononuclearity throughout complex catalytic cycles,[3] to promote metal–metal bond formation in homo- and heterobimetallic complexes,[4] and to control the nature of the second coordination sphere.[5]

We were interested in combining the high stability of the tripodal framework with the redox activity of amidophenolate ligands. Amidophenolates have attracted attention for their ability to engage in ligand-centered redox activity, forming monoanionic iminosemiquinonate or neutral iminoquinones when bonded to transition or main group metals. Such ligands have been used as electron reservoirs to enable oxidative addition[6] or reductive elimination[7] reactions of early transition metals.

We have previously studied molybdenum complexes of the 2,2′-biphenyl-bridged bis(amidophenoxide) ligand ^{t}BuClip^{4-} (^{t}BuClipH$_4$ = 4,4′-di-*tert*-butyl-*N*,*N*′-bis(3,5-di-*tert*-butyl-2-hydroxyphenyl)-2,2′-diaminobiphenyl) containing ancillary terminal oxo, bridging nitrido, and alkoxide ligands.[8] These compounds do undergo ligand-centered oxidation reactions. More significantly, the high-lying ligand orbital responsible for the redox-activity is also capable of strong π donation to molybdenum(VI). This has important structural consequences, for example determining the isomers favored in oxo[9,10] and nitrido complexes. The π donor ability also appears to have chemical consequences, for example allowing the replacement of all oxo ligands in oxomolybdenum(VI) reagents.[11,12]

Here we describe the preparation of a novel tripodal ligand, tris(2-(3′,5′-di-*tert*-butyl-2′-hydroxyphenyl)amino-4-methylphenyl)-amine, MeClampH$_6$, in which the three arms emanating from the central triarylamine donor are *o*-aminophenols. The fully deprotonated MeClamp^{6-} forms a very stable seven-coordinate tris(amidophenolate) complex with molybdenum(VI) which undergoes ligand-centered oxidations. Furthermore, the spectroscopy of the complex can be used to make a rare semiquantitative estimate of the stabilization of the complex due specifically to π bonding.

Experimental

General procedures

Unless otherwise noted, all procedures were carried out on the benchtop without precautions to exclude air or moisture. NMR spectra were measured on Varian VXR-300 or Bruker Avance DPX 400 spectrometers. Chemical shifts for ^{1}H and ^{13}C{^{1}H} spectra are reported in ppm downfield of TMS, with spectra referenced using the known chemical shifts of the solvent residuals. Infrared spectra were recorded by ATR on a Jasco 6300 FT-IR spectrometer. UV-Visible spectra were

Department of Chemistry and Biochemistry, 251 Nieuwland Science Hall; University of Notre Dame, Notre Dame, IN 46556-5670, USA.
E-mail: Seth.N.Brown.114@nd.edu; Fax: +1 574 631 6652; Tel: +1 574 631 4659

†Electronic supplementary information (ESI) available: Energy and Cartesian coordinates for calculated structures of (Clamp)Mo and (Clamp)Mo$^+$ and TDDFT calculations for (Clamp)Mo. CCDC 1023169–1023170. For ESI and crystallographic data in CIF or other electronic format see DOI: 10.1039/c4dt02936d

recorded in 1 cm quartz cells on a Beckman DU-7500 or a ThermoFisher Evolution Array diode array spectrophotometer. ESI mass spectra were obtained using a Bruker micrOTOF-II mass spectrometer, and peaks reported are the mass number of the most intense peak of isotope envelopes. Elemental analyses were performed by Robertson Microlit Labs (Ledgewood, NJ) or M-H-W Laboratories (Phoenix, AZ).

Syntheses

Tris(2-nitro-4-methylphenyl)amine, N(C_6H_3-2-NO_2-4-CH_3)$_3$. This compound is prepared by a variation of a previous procedure[13] that avoids chromatography and produces the desired material in high yield. Into a 250 mL Erlenmeyer flask is weighed tri-*p*-tolylamine (TCI, 1.85 g, 6.44 mmol). Acetic anhydride (75 mL) is added and the mixture stirred until most of the solid dissolves. To the stirred mixture is added $Cu(NO_3)_2{\cdot}2.5\ H_2O$ (3.00 g, 12.9 mmol, 2.00 equiv.) and the flask is sealed with parafilm. The solution is initially blue and then turns a brownish green with a green precipitate. After stirring 2 h, the mixture is poured into 300 mL H_2O and stirred overnight. The brownish-orange solid is isolated by suction filtration on a glass frit, washed thoroughly with 2 × 30 mL H_2O and 3 × 20 mL CH_3OH, and air-dried 1 h to yield 2.20 g tris(2-nitro-4-methylphenyl)amine as a yellow powder (82%). ^{1}H NMR ($CDCl_3$): δ 2.37 (s, 9H, CH_3), 7.05 (d, 8 Hz, 3H, ArH-6), 7.29 (dd, 8, 1.5 Hz, 3H, ArH-5), 7.61 (d, 1.5 Hz, 3H, ArH-3). ^{13}C{^{1}H} NMR ($CDCl_3$): δ 20.88 (CH_3), 126.49, 128.20, 134.77, 136.33, 136.80, 143.62. IR (cm^{-1}): 3066 (w), 2922 (w), 1614 (w), 1564 (w), 1526 (vs, ν_{as}, NO_2), 1499 (s), 1453 (w), 1403 (w), 1385 (w), 1346 (vs, ν_{sym}, NO_2), 1281 (s), 1250 (s), 1218 (w), 1189 (w), 1154 (m), 1092 (w), 1038 (w), 919 (w), 889 (w), 829 (m), 801 (m), 763 (w), 706 (w), 601 (w). ESI-MS: 445.1107 (M + Na, calcd 445.1124). Anal. Calcd for $C_{21}H_{18}N_4O_6$: C, 59.71; H, 4.30; N, 13.26. Found: C, 59.78; H, 4.49; N, 13.11.

Tris(2-amino-4-methylphenyl)amine, N(C_6H_3-2-NH_2-4-CH_3)$_3$. In a 50 mL round-bottom flask, 158.0 mg tris(2-nitro-4-methylphenyl)amine (0.374 mmol) is dissolved in 4 mL THF. 15 mL methanol is added and upon stirring, a precipitate forms. To the stirred slurry is added 344.6 mg CuCl (3.48 mmol, 9.3 equiv.) in a single portion, followed by 430.4 mg KBH_4 (7.98 mmol, 21.3 equiv.) in small portions over 5 min. After vigorous gas evolution, the solution turns brown, but becomes colourless with a coarse black precipitate about 6 min after complete borohydride addition. After stirring 25 min, the mixture is suction filtered and the precipitate washed with 20 mL ethyl acetate. The filtrate is stripped down on the rotary evaporator and partitioned between 30 mL each of ethyl acetate and water. After removing the water layer, the EtOAc layer is washed with dilute aqueous sodium dithionite followed by brine and dried over $MgSO_4$. After removing the EtOAc on the rotary evaporator, the residue is slurried in 5 mL CH_3OH and isolated by suction filtration. Washing the solid with 5 mL CH_3OH and air-drying 20 min furnishes 78.3 mg triamine as a grey-white solid (62%). ^{1}H NMR ($CDCl_3$): δ 2.24 (s, 9H, CH_3), 3.64 (br s, 6H, NH_2), 6.50 (sl br dd, 8, 2.5 Hz, 3H, ArH-5), 6.53 (s, 3H, ArH-3), 6.79 (d, 8 Hz, 3H, ArH-6). ^{13}C{^{1}H} NMR ($CDCl_3$): δ 21.28 (CH_3), 117.21, 119.74, 125.40, 130.55, 135.27, 141.09. IR (cm^{-1}): 3455 (m, ν_{NH}), 3368 (m, ν_{NH}), 2952 (w), 2916 (w), 2859 (w), 1736 (w), 1611 (m), 1574 (w), 1506 (s), 1455 (w), 1427 (w), 1304 (m), 1234 (s), 1195 (w), 1172 (w), 1137 (w), 951 (w), 865 (w), 850 (w), 808 (m), 739 (w), 596 (w). ESI-MS: 333.2119 (M + H, calcd 333.2080). Anal. Calcd for $C_{21}H_{24}N_4$: C, 75.87; H, 7.28; N, 16.85. Found: C, 76.19; H, 7.04; N, 17.00.

Tris(2-(3′,5′-di-*tert*-butyl-2′-hydroxyphenyl)amino-4-methylphenyl)amine, MeClampH$_6$. In a 50 mL round-bottom flask, 403.7 mg tris(2-amino-4-methylphenyl)amine (1.21 mmol) and 809.9 mg 3,5-di-*tert*-butylcatechol (Aldrich, 3.64 mmol, 3.0 equiv.) are added to 20 mL hexanes and 200 μL glacial acetic acid. The flask is sealed with parafilm and the mixture is stirred for 2 d. The dark brown slurry is filtered on a glass frit and the solid washed thoroughly with 6 × 6 mL CH_3OH to remove colored impurities. The solid is air-dried 1 h to yield 829.2 mg MeClampH$_6$ (72%). ^{1}H NMR ($CDCl_3$): δ 1.09 (s, 27H, ^{t}Bu), 1.36 (s, 27H, ^{t}Bu), 2.20 (s, 9H, CH_3), 5.38 (br s, 3H, NH), 6.02 (s, 3H, OH), 6.40 (d, 1.5 Hz, 3H, ArH-3), 6.49 (d, 2 Hz, 3H, ArH-4′), 6.67 (dd, 8, 1.5 Hz, 3H, ArH-5), 6.98 (d, 8 Hz, 3H, ArH-6), 7.10 (d, 2 Hz, 3H, ArH-6′). ^{13}C{^{1}H} NMR ($CDCl_3$): δ 21.56 (ArCH_3), 29.76, 31.62 (C(CH_3)$_3$), 34.41, 35.13 (C(CH_3)$_3$), 116.81, 121.26, 121.42, 121.91, 124.91, 128.09, 131.42, 135.63, 136.44, 140.87, 142.45, 149.09. IR (cm^{-1}): 3456 (w, ν_{OH}), 3374 (w, ν_{NH}), 2952 (m), 2868 (w), 1608 (w), 1577 (w), 1510 (w), 1485 (m), 1460 (w), 1420 (m), 1391 (w), 1362 (m), 1336 (w), 1309 (m), 1254 (w), 1213 (m), 1196 (m), 1161 (w), 1121 (w), 1023 (w), 978 (w), 880 (w), 818 (w), 798 (m), 739 (w), 712 (w), 660 (m), 624 (m), 595 (w). ESI-MS: 941.6319 (M$^+$ − 3H, calcd 941.6309). Anal. Calcd for $C_{63}H_{84}N_4O_3$: C, 80.04; H, 8.96; N, 5.93. Found: C, 79.81; H, 8.72; N, 5.82.

κ^7-[Tris(2-(3′,5′-di-*tert*-butyl-2′-oxyphenyl)amido-4-methylphenyl)amine]molybdenum(VI), (MeClamp)Mo. In the drybox, 0.1131 g MeClampH$_6$ (0.1196 mmol) and 0.0595 g MoO_2(acac)$_2$ (0.184 mmol, 1.5 equiv.) are dissolved in 4 mL CH_2Cl_2 and allowed to stand 36 h at room temperature. During this time the solution changes from dark brown to deep purple. In the air, the solvent is removed on the rotary evaporator and the black residue is slurried with 5 mL acetonitrile and vacuum filtered through a glass frit. The solid is washed with 5 mL CH_3CN and air-dried 15 min to yield 46.1 mg (MeClamp)Mo (37%). ^{1}H NMR ($CDCl_3$, with added trace of Cp*$_2$Fe): δ 1.22 (s, 27H, ^{t}Bu), 1.31 (s, 27H, ^{t}Bu), 2.29 (s, 9H, CH_3), 6.56 (sl br dd, 8, 2 Hz, 3H, ArH-5), 6.81 (d, 8 Hz, 3H, ArH-6), 6.88 (d, 2 Hz, 3H, ArH-4′), 7.23 (s, 3H, ArH-3), 7.29 (d, 2 Hz, 3H, ArH-6′). ^{13}C{^{1}H} NMR (CD_2Cl_2, with added trace of Cp*$_2$Fe): δ 22.08 (ArCH_3), 30.29, 32.01 (C(CH_3)$_3$), 35.15, 35.53 (C(CH_3)$_3$), 107.51, 119.09, 119.36, 122.33, 123.35, 128.86, 138.06, 140.08, 142.50, 143.63, 144.35, 147.34. IR (cm^{-1}): 2952 (s), 2903 (m), 2867 (m), 1588 (m), 1490 (s), 1457 (m), 1421 (m), 1409 (m), 1388 (w), 1360 (m), 1343 (w), 1305 (s), 1281 (w), 1260 (m), 1232 (m), 1201 (m), 1171 (m), 1000 (m), 945 (m). ESI-MS: 1036.4996 (M + H, calcd 1036.3099). UV-Vis (CH_2Cl_2): λ_{max} = 295 nm (sh, ε = 19 500 L mol^{-1} cm^{-1}), 356 (12 000), 513 (sh, 8500), 563 (10 700), 985 nm (6900). Anal. Calcd for $C_{63}H_{78}MoN_4O_3$: C, 73.09; H, 7.59; N, 5.41. Found: C, 70.19; H, 7.38; N, 5.10.

Electrochemistry

Cyclic voltammograms were performed at a scan rate of 120 mV s^{-1} using a BAS Epsilon potentiostat, with glassy carbon working and counter electrodes and a silver/silver chloride pseudo-reference electrode. The electrodes were connected to the potentiostat through electrical conduits in the drybox wall. The sample of (MeClamp)Mo was 1 mM in CH_2Cl_2, with 0.1 M Bu_4NPF_6 as the electrolyte. Potentials were referenced to ferrocene/ferrocenium at 0 V,[14] with the reference potential established by spiking the test solution with a small amount of ferrocene.

DFT calculations

Geometry optimizations and orbital calculations were performed using the crystal structure of (MeClamp)Mo as a starting structure, and with all *tert*-butyl groups and methyl groups replaced with hydrogens. Calculations used the hybrid B3LYP method, with an SDD basis set for molybdenum and a 6-31G* basis set for all other atoms, using the Gaussian09 suite of programs.[15] The optimized geometries were confirmed as minima by calculation of vibrational frequencies. Plots of calculated Kohn–Sham orbitals were generated using Gaussview (v. 5.0.8) with an isovalue of 0.04.

X-ray crystallography

Crystals of (MeClamp)Mo·CH_3CN were grown by slow evaporation of acetonitrile solutions while crystals of (MeClamp)Mo·$3C_6H_6$ were grown by layering a concentrated 10 : 1 dichloromethane–hexane solution with benzene. Crystals were placed in inert oil before being transferred to the cold N_2 stream of a Bruker Apex II CCD diffractometer. Data were reduced, correcting for absorption, using the program SADABS. The structures were solved using direct methods. All nonhydrogen atoms not apparent from the initial solutions were found on difference Fourier maps, and all heavy atoms were refined anisotropically. In the acetonitrile solvate, two *tert*-butyl groups (those attached to C28 and C68) were refined in two alternate orientations, with opposing methyl groups constrained to have the same thermal parameters. The minor components refined to 12.6(5)% and 12.4(5)% occupancy, respectively. Hydrogen atoms on the metal complex in the benzene solvate were located on difference maps and refined isotropically, while all other hydrogen atoms were placed in calculated positions, with thermal parameters for the hydrogens tied to the isotropic thermal parameters of the atoms to which they are bonded (1.5× for methyl, 1.2× for others). Calculations used SHELXTL (Bruker AXS),[16] with scattering factors and anomalous dispersion terms taken from the literature.[17] Further details about the structures are in Table 1.

Table 1 Crystal data for (MeClamp)Mo·CH_3CN and (MeClamp)Mo·$3C_6H_6$

	(MeClamp)Mo·CH_3CN	(MeClamp)Mo·$3C_6H_6$
Molecular formula	$C_{65}H_{81}MoN_5O_3$	$C_{81}H_{96}MoN_4O_3$
Formula weight	1076.29	1269.56
T/K	120(2)	120(2)
Crystal system	Monoclinic	Rhombohedral
Space group	$P2_1/c$	$R\bar{3}$
λ/Å	0.71073 (Mo Kα)	0.71073 (Mo Kα)
Total data collected	194 202	48 841
No. of indep reflns	24 403	5931
R_{int}	0.1778	0.0255
Obsd refls [$I > 2\sigma(I)$]	13 890	5380
a/Å	20.1764(12)	17.2078(5)
b/Å	46.334(3)	17.2078(5)
c/Å	12.7362(7)	17.2078(5)
α/°	90	60.5230(10)
β/°	94.734(4)	60.5230(10)
γ/°	90	60.5230(10)
V/Å^3	11 866.0(12)	3645.56(18)
Z	8	2
μ/mm^{-1}	0.269	0.229
Crystal size/mm	0.35 × 0.14 × 0.04	0.58 × 0.35 × 0.21
No. refined params	1361	372
R_1, wR_2 [$I > 2\sigma(I)$]	R_1 = 0.0574, wR_2 = 0.1137	R_1 = 0.0308, wR_2 = 0.0826
R_1, wR_2 [all data]	R_1 = 0.1305, wR_2 = 0.1400	R_1 = 0.0360, wR_2 = 0.0874
Goodness of fit	0.986	0.969

Results and discussion

Synthesis of the tris(aminophenol) MeClampH$_6$

Chelating bis(aminophenol) ligands have been prepared previously with aromatic (1,2-benzenediyl[18] or 2,2-biphenyldiyl[8,19,20]) or aliphatic[21] linkers bridging the two nitrogen atoms. A chelating tris(aminophenol) ligand had not been previously prepared, but we anticipated that one would be able to bind to a single metal in a hexa- or heptadentate fashion based on six- and seven-coordinate molybdenum bis(amidophenolate)-catecholates[11] and on numerous examples of octahedral tris(iminosemiquinonates).[22]

The tris(aminophenol) ligand designated MeClampH$_6$ is prepared in three steps from commercially available tri-*p*-tolylamine (Scheme 1), with the three aminophenols attached to the *ortho* positions of the tritolylamine. Tris(2-aminophenyl)-amine has been prepared previously[23] and has been success-

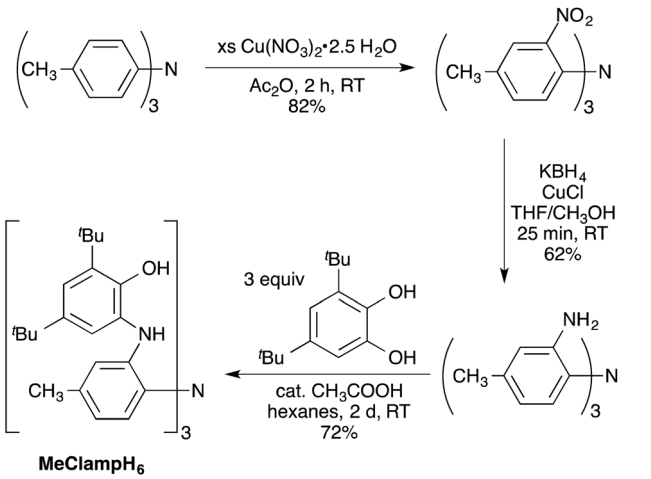

Scheme 1 Synthesis of MeClampH$_6$.

fully elaborated into tripodal ligands.[24] The use of the methyl substituent *para* to the central nitrogen in the present synthesis allows one to avoid the cumbersome nucleophilic aromatic substitution used to assemble the unsubstituted compound. Furthermore, *para*-substitution of triarylamines is known to greatly increase the stability of their radical cations,[25] which may be important if the ligand or its complexes are to be investigated under oxidative conditions.

Tri-*p*-tolylamine is readily nitrated with excess copper(II) nitrate in acetic anhydride to furnish the trinitro compound $N(C_6H_3\text{-}2\text{-}NO_2\text{-}4\text{-}CH_3)_3$. This nitration was previously described by Fry and coworkers to give the compound as a mixture that required chromatographic separation from products of partial nitration.[13] We find that use of a modest excess of copper nitrate (2 mol per mol triarylamine) suffices to drive the reaction to completion, and the desired product can be isolated by filtration of the reaction mixture in good yield and high purity. Reduction of the nitro groups to the triamine is accomplished using $KBH_4/CuCl$,[26] a method that has previously been employed for the reduction of *o*-nitro-*N*-arylanilines.[27] Hydrogenation over 10% Pd/C is also successful, but the reaction is slower and yields are lower. Condensation of the triamine proceeds smoothly in the presence of catalytic acetic acid to afford the desired tris(aminophenol), $MeClampH_6$, in good yield after filtration and washing with methanol. Triethylamine has been more commonly used as a catalyst in this condensation reaction,[8,20,28] but is ineffective here.

Synthesis and structure of (MeClamp)Mo

Commercially available oxomolybdenum(VI) bis(acetylacetonate), $MoO_2(acac)_2$, has been used as a convenient starting material for the preparation of catecholate and amidophenolate complexes containing zero,[11,12] one[10,29] or two[8] remaining oxo groups. The hexaprotic ligand $MeClampH_6$ reacts with $MoO_2(acac)_2$ over the course of 36 h to produce oxo-free, air-stable, dark purple (MeClamp)Mo (eqn (1)),

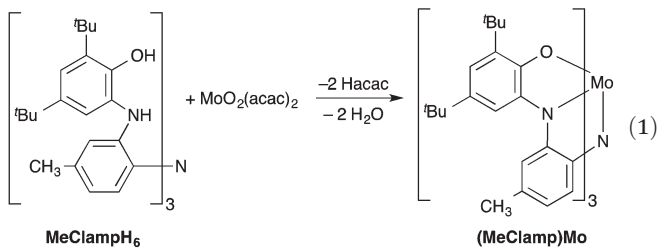

MeClampH$_6$ **(MeClamp)Mo** (1)

which can be isolated by precipitation from acetonitrile. Production of free Hacac is observed *in situ* by ^{1}H NMR spectroscopy. Loss of both oxo ligands is suggested by the mass spectrum (which shows a parent ion at m/z = 1036) and the lack of an oxo stretch in the IR spectrum. ^{1}H NMR spectra of the as-prepared material are appreciably broadened, as we[30] and others[31] have sometimes observed in complexes with easily oxidized ligands, where a minute amount of the radical cation can rapidly undergo electron transfer with the neutral compound and broaden the entire spectrum. Addition of a trace of decamethylferrocene reduces any adventitiously oxidized material, and results in sharp ^{1}H and $^{13}C\{^1H\}$ NMR spectra with peaks corresponding to a symmetrical ligand at normal, diamagnetic chemical shifts.

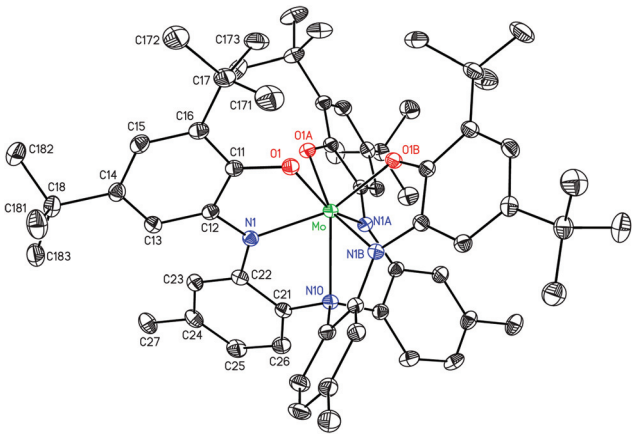

Fig. 1 Thermal ellipsoid plot (50% ellipsoids) of the metal complex in (MeClamp)Mo·3C_6H_6. Hydrogen atoms are omitted for clarity.

The solid-state structure of (MeClamp)Mo was determined by X-ray crystallographic analysis of the complex as both a benzene and an acetonitrile solvate (Table 1). The molecular structure of the complex is essentially identical in both crystals (Fig. 1, Table 2), and is seven-coordinate, adopting a C_3-symmetric, capped octahedral structure with the triarylamine nitrogen supplying the capping ligand. This is very similar to the structure adopted by (3,5-^{t}Bu$_2$Cat)$_3$Mo(py),[32] and the Mo–NAr_3 distance of 2.28 Å (Table 2) is close to the Mo–py distance of 2.274(2) Å in the tris(catecholate) structure. Heptadentate coordination of anionic tripodal ligands is well known for lanthanides[33] and main group elements,[34] but is uncommon for transition metals.[35]

The intraligand bond distances in amidophenoxides and related catecholates have been used extensively to gauge the degree of oxidation of the ligand.[36] Given the diamagnetism of the compound, a formal oxidation state of +6 for molybdenum with fully reduced amidophenoxide ligands seems chemically secure. Analysis of the bond distances using established correlations[37] gives an apparent metrical oxidation state (MOS) of −1.52(9), averaged between the values in the two crystal structures (Table 2). Such noninteger values of the MOS do not generally map onto formal oxidation states (which would require a Mo oxidation state of 4.5 in this case), and instead are most sensibly interpreted in terms of π bonding,[37,38] with the decrease in electron density in the amidophenolate HOMO due to π donation to the Mo center causing bond distance changes akin to those caused by outright oxidation of the amidophenoxide. The MOS values observed for (MeClamp)Mo are typical of other molybdenum(VI) amidophenoxides.[8,11]

Outer-sphere redox chemistry of (MeClamp)Mo

Inner-sphere oxygen atom donors such as amine-*N*-oxides do not react with (MeClamp)Mo, in contrast to their behavior toward Mo(VI) catecholate complexes.[10,32] Presumably this is

Table 2 Selected bond distances (Å), metrical oxidation states and angles (°) in (MeClamp)Mo (X-ray), (Clamp)Mo (DFT) and (Clamp)Mo^+ (DFT)

	X-ray (MeClamp)Mo·3C_6H_6	X-ray[a] (MeClamp)Mo·CH_3CN	DFT[b] (Clamp)Mo	DFT[b] (Clamp)Mo^+
Mo–O1	2.0077(9)	1.994(16)	2.016	2.032
Mo–N1	2.0726(11)	2.066(17)	2.102	2.111
Mo–N10	2.2940(19)	2.273(15)	2.340	2.344
C11–O1	1.3300(16)	1.334(6)	1.324	1.312
C12–N1	1.3778(17)	1.381(10)	1.379	1.362
C11–C12	1.4120(18)	1.408(8)	1.424	1.438
C12–C13	1.4076(19)	1.397(9)	1.410	1.419
C13–C14	1.3815(19)	1.384(7)	1.391	1.381
C14–C15	1.413(2)	1.405(7)	1.407	1.419
C15–C16	1.388(2)	1.384(6)	1.389	1.383
C16–C11	1.4168(18)	1.404(8)	1.403	1.408
MOS	−1.47(5)	−1.58(6)	−1.47(7)	−1.20(6)
O1–Mo–O1A	83.42(4)	83(3)	84.0	85.4
O1–Mo–N1	74.49(4)	74.6(6)	74.5	74.4
O1–Mo–N1A	157.17(4)	157(2)	157.8	158.8
O1–Mo–N1B	88.32(4)	88(2)	87.9	86.5
O1–Mo–N10	129.80(3)	130(3)	129.4	128.5
N1–Mo–N1A	109.95(3)	110(5)	109.8	110.1
N1–Mo–N10	71.01(3)	71.2(7)	70.9	71.1
C21–N10–Mo	106.00(9)	106.5(12)	105.4	105.4
C21–N10–C21A	112.71(8)	112.3(14)	113.2	113.3
C12–N1–Mo	118.26(9)	118(2)	117.5	117.8
C22–N1–Mo	116.69(9)	117.0(8)	116.0	115.6
C12–N1–C22	124.61(11)	124.8(13)	125.9	126.3
C11–O1–Mo	119.86(8)	119.8(13)	119.7	119.5

[a] Values represent averages over chemically equivalent examples in the two crystallographically unique molecules of (MeClamp)Mo; esd's include the variation among the observations as well as the statistical uncertainty of the fit. [b] Structure optimization (B3LYP; SDD basis for Mo, 6-31G* for all others) performed on compound with all ^{t}Bu and CH_3 groups replaced with H.

because the heptadentate chelation blocks access to the molybdenum. This multidentate chelation stabilizes the metal as it undergoes outer-sphere redox chemistry, leading to the observation of three reversible waves in the cyclic voltammogram of (MeClamp)Mo (Fig. 2). The two waves at −0.17 and +0.55 V *vs.* Fc^+/Fc are attributed to amidophenolate-centered oxidations, and the reduction at −1.40 V is Mo-centered (free tri-*p*-tolylamine oxidizes at +0.33 V,[39] but coordination of the amine to molybdenum will make this oxidation much more difficult).

The monocation $[(MeClamp)Mo]^+$ is generated in solution by treatment with chemical oxidants such as ferrocenium hexafluorophosphate. Titration of (MeClamp)Mo with $[Cp_2Fe]PF_6$ generates a new optical spectrum with clean isosbestic points and requires 1.0 equiv. of oxidant for complete reaction (Fig. 3). EPR spectroscopy of solutions of *in situ* generated $[(MeClamp)Mo]^+$ at room temperature shows a strong signal with no discernible hyperfine coupling at $g = 2.016$, consistent with a ligand-centered radical. Similar EPR behavior is observed in oxidized ruthenium and osmium tris(amidophenolate) complexes.[22f,h]

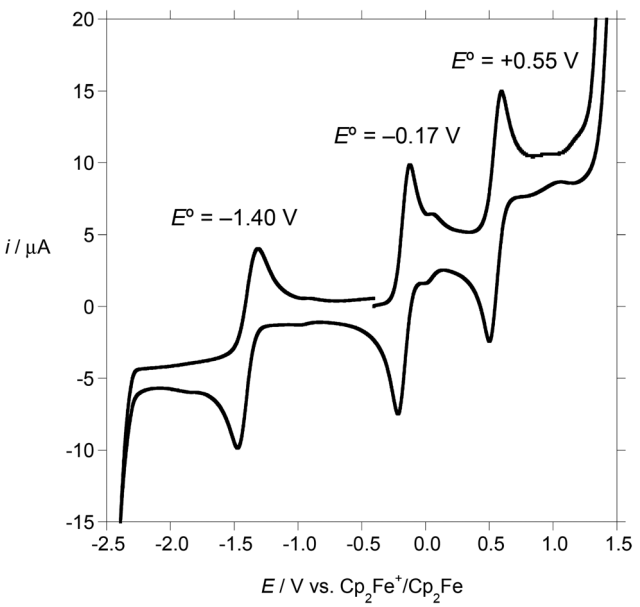

Fig. 2 Cyclic voltammogram of (MeClamp)Mo in CH_2Cl_2 (0.1 M Bu_4NPF_6, 120 mV s^{-1}).

π Bonding in (MeClamp)Mo

The intraligand bond lengths in (MeClamp)Mo show evidence of significant amidophenolate-to-metal π donation. Density functional theory calculations on (Clamp)Mo (with the *tert*-butyl and methyl groups replaced by hydrogen) support the presence of strong π bonding. Calculations converge on a C_3-symmetric minimum-energy structure whose geometry is strikingly similar to experimental observations (with the exception of a slight overestimate of the metal–nitrogen distances by theory, Table 2). In particular, DFT captures the intraligand distances faithfully, giving an MOS value of −1.47(7), in excellent agreement with experiment.

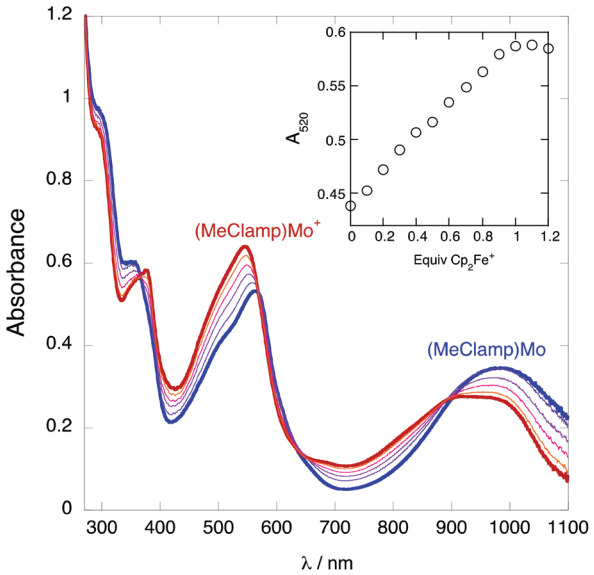

Fig. 3 UV-Vis-NIR titration of (MeClamp)Mo (5×10^{-5} M, CH_2Cl_2) with $[Cp_2Fe]PF_6$. Scans are shown every 0.2 equiv. Cp_2Fe^+ from 0 to 1.0 equiv. Inset: Absorbance at 520 nm as a function of added $[Cp_2Fe]PF_6$.

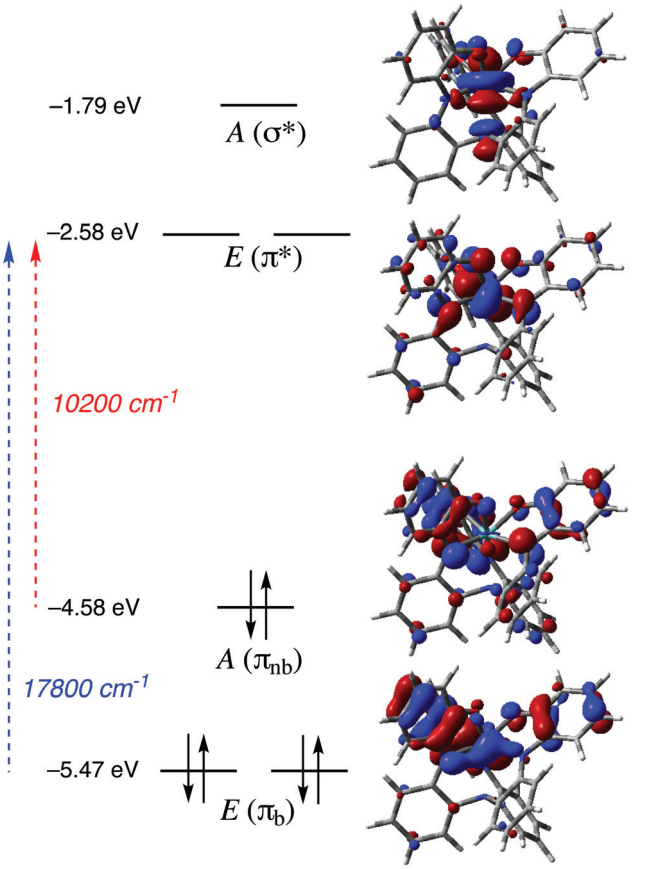

Fig. 4 MO diagram of C_3-symmetric (MeClamp)Mo, with methyl and *tert*-butyl groups replaced by hydrogen. Energies are calculated for the corresponding Kohn–Sham orbitals (B3LYP, 6-31G*/SDD for Mo). Frequencies are from the experimentally measured optical transitions. Only one orbital from each *E* set is pictured.

The three ligand-centered redox-active orbitals split into an *E* set and an *A* combination in C_3 symmetry (Fig. 4). Of these, the *E* orbitals interact strongly with the Mo dπ orbitals and form a bonding and an antibonding combination. The *A* symmetry ligand-centered combination has little overlap with the metal d_{z^2} orbital (its only symmetry match among the d orbitals) and is essentially nonbonding. This analysis is essentially the same as in other threefold symmetric metal complexes with three (σ + 2π) ligands; familiar examples include $(\eta^5\text{-}C_5H_5)_3ZrX$,[40] $(RCCR)_3W(L)$,[41] and $(RN)_3WL$.[42]

There is thus a formal π bond order of 2 in (MeClamp)Mo, delocalized over the three amidophenolate ligands. This is in good agreement with the structural data. For comparison, in the oxobis(amidophenolate) complex (^{t}BuClip)MoO(3,5-lut), one amidophenolate must compete with the oxo ligand for π bonding to the molybdenum and has a π bond order of zero (MOS = −2.00(9)), while the other amidophenolate donates into a strictly nonbonding dπ orbital and has a π bond order of one (MOS = −1.34(12)). The amidophenolates in (MeClamp)Mo, with a π bond order of 2/3, have MOS values (−1.52(9)) two-thirds of the way between these two values.

According to the MO analysis, oxidation of (MeClamp)Mo should cause loss of an electron from the *A*-symmetry, π nonbonding orbital and would give a delocalized but ligand-centered radical. This is consistent with the relatively facile oxidation of (MeClamp)Mo (E° = −0.17 V *vs.* ferrocene/ferrocenium) and with the EPR spectrum of the cation. It is also supported by DFT calculations on the cation, which show only small changes in bond distances and angles (Table 2); the MOS becomes more positive overall by 0.81, suggesting that the degree of π bonding has not changed substantially. The small changes in geometry and delocalization of charge suggest a small reorganization energy for the (MeClamp)Mo/(MeClamp)Mo$^+$ redox couple, predicting rapid degenerate electron transfer, consistent with the experimental observation that even traces of the cation strongly broaden the NMR spectra of the neutral species.

If the π bonding is strong enough, one would predict that the dication would lose the second electron from the *A* orbital to form a delocalized singlet bis(iminosemiquinone) species. The second oxidation (at +0.55 V) is at a low enough potential to suggest that this is plausible; in (^{t}BuClip)MoO(py), the π-nonbonding amidophenolate is oxidized at +0.06 V, but the π-bonded amidophenolate is not oxidized below +1.1 V.[8] Unfortunately, we have been unable to generate stable solutions of (MeClamp)Mo^{2+}, so no experimental data are available to address its bonding.

The π bonding of the neutral (MeClamp)Mo can be addressed through an analysis of its optical spectrum. In their seminal study of the optical spectra of iron(III)[43] and vanadium(IV)[44] tris(catecholates), Solomon and Raymond noted that the difference in energy in the two lowest-energy charge-transfer bands, the a_2 (Cat π_{nb}) → e (dπ*) and e (Cat π_b) → e (dπ*), cor-

responded to the difference in energy of the catecholate orbitals caused by metal–ligand π bonding (a value they called γ). The bonding picture in (MeClamp)Mo is similar to that of a metal tris(catecholate), with the exception that d_{z^2}, which is strictly nonbonding in the octahedral D_3-symmetric tris(catecholate), is substantially raised in energy in (Clamp)Mo due to its strong σ* interaction with the central triarylamine. The two lowest-energy transitions observed in the optical spectrum of (MeClamp)Mo are at 10 200 and 17 800 cm^{-1}, and TDDFT calculations support their assignment as being due to the a (π_{nb}) → e (π*) and e (π_b) → e (π*) transitions, respectively, with calculated transitions at 11 400 and 18 100 cm^{-1}, respectively. Thus, for (MeClamp)Mo, γ = 7600 cm^{-1} (0.94 eV), which is in excellent agreement with the difference in the calculated energies of the respective Kohn–Sham orbitals (0.89 eV). Unsurprisingly, the π bonding in this Mo(VI) tris(amidophenoxide) is substantially stronger than that seen in Fe(III) (γ = 3600 cm^{-1})[43] or V(IV) (γ = 3900 cm^{-1})[44] tris(catecholate) complexes. The difference likely originates from greater basicity of amidophenolates relative to catecholates, the higher oxidation state of molybdenum, and the fact that Mo is a second-row transition metal.

Equating γ to the stabilization afforded to the ligand by π bonding to the metal neglects any effects caused by different electron-electron repulsion terms in the excited states. In $[Fe(Cat)_3]^{3-}$, this neglect was justified by the fact that the donor orbitals were ligand-localized and the acceptor orbital metal-localized.[43] That assumption should still be roughly true in (MeClamp)Mo, though the increased covalency and orbital mixing in this compound does make this approximation less exact. With this caveat in mind, one can translate the one-electron energy γ = 7600 cm^{-1} to an estimate that each of the (two-electron) π bonds formed by the amidophenolates contributes roughly 40 kcal mol^{-1} to the overall stability of the molecule. Such quantitative experimental estimates of the π component of bonding are extremely rare, especially for strongly π bonding ligands; they are only possible in this case due to the presence of analogous ligand nonbonding orbitals to serve as a sort of internal standard. Computationally, dissecting interactions into σ and π components is more tractable, and has been carried out by methods such as energy decomposition analysis, which allows one to partition bonding stabilization into σ and π components (when these are of different irreducible representations).[45] Such an analysis, when applied to $MoOCl_4$, furnishes an estimate of 36 kcal mol^{-1} of stabilization energy for each Mo–O π bond.[46] Since this value is derived from combination of singlet $MoCl_4$ with an O atom in the $(p\sigma)^0(p\pi)^4$ configuration, it represents a donor–acceptor interaction that should be analogous to the experimental estimate obtained here for amidophenoxides,[47] though quantitative comparison of values obtained by such different methods is problematic. Nevertheless, based on the data obtained here, the amidophenoxide ligand is clearly a strong π donor. This is undoubtedly an important factor in the amidophenolate's unusual ability to replace all the oxo groups in molybdenum(VI) compounds.[8,11,12]

Conclusions

A C_3-symmetric tris(aminophenol) ligand with the amino groups bonded to the *ortho* positions of a triarylamine, $MeClampH_6$, is prepared in three steps from tri-*p*-tolylamine. It is metalated by $MoO_2(acac)_2$ to form oxo-free (MeClamp)Mo, in which the ligand is heptadentate, binding through all three amidophenolates and through the neutral amine nitrogen. Structural data and DFT calculations indicate that the compound is well described as molybdenum(VI) bound to fully reduced amidophenolates, with strong π donation to molybdenum from the *E* combination of amidophenolate orbitals. Analysis of the optical spectrum, using the essentially nonbonding *A* combination of amidophenolate orbitals as a benchmark, allows one to estimate the energetic stabilization of the ligand donor orbitals due to π bonding as about 0.9 eV, corresponding to roughly 40 kcal mol^{-1} for each π bond.

Acknowledgements

This work was generously supported by a grant from the US National Science Foundation (CHE-1112356). T. M.-R. acknowledges fellowship support from the Notre Dame College of Science COS-SURF program, and from a Vincent Slatt Fellowship administered by the Center for Sustainable Energy at Notre Dame. We thank Dr Allen G. Oliver for assistance with the X-ray crystallography and Dr Jaroslav Zajicek for assistance with the EPR spectroscopy.

Notes and references

1 (*a*) C. C. Cummins, J. Lee, R. R. Schrock and W. D. Davis, *Angew. Chem., Int. Ed. Engl.*, 1992, **31**, 1501–1503; (*b*) M. Ray, B. S. Hammes, G. P. A. Yap, A. L. Rheingold and A. S. Borovik, *Inorg. Chem.*, 1998, **37**, 1527–1532; (*c*) C. E. Searls, S. T. Kleespies, M. L. Eppright, S. C. Schwartz, G. P. A. Yap and R. C. Scarrow, *Inorg. Chem.*, 2010, **49**, 11261–11263.

2 (*a*) T. Kemmitt, N. I. Al-Salim, G. J. Gainsford and W. Henderson, *Aust. J. Chem.*, 1999, **52**, 915–919; (*b*) V. Ugrinova, G. A. Ellis and S. N. Brown, *Chem. Commun.*, 2004, 468–469.

3 R. R. Schrock, *Acc. Chem. Res.*, 2005, **38**, 955–962.

4 (*a*) S. T. Liddle, J. McMaster, D. P. Mills, A. J. Blake, C. Jones and W. D. Woodul, *Angew. Chem., Int. Ed.*, 2009, **48**, 1077–1080; (*b*) P. A. Rudd, S. Liu, N. Planas, E. Bill, L. Gagliardi and C. C. Lu, *Angew. Chem., Int. Ed.*, 2013, **52**, 4449–4452; (*c*) C. M. Zall, L. J. Clouston, V. G. Young, K. Ding, H. J. Kim, D. Zherebetskyy, Y.-S. Chen, E. Bill, L. Gagliardi and C. C. Lu, *Inorg. Chem.*, 2013, **52**, 9216–9228; (*d*) S. J. Tereniak, R. K. Carlson, L. J. Clouston, V. G. Young, E. Bill, R. Maurice, Y.-S. Chen, H. J. Kim, L. Gagliardi and C. C. Lu, *J. Am. Chem. Soc.*, 2014, **136**, 1842–1855.

5 (*a*) R. L. Lucas, M. K. Zart, J. Mukherjee, T. N. Sorrell, D. R. Powell and A. S. Borovik, *J. Am. Chem. Soc.*, 2006, **128**, 15476–15489; (*b*) D. Natale and J. C. Mareque-Rivas, *Chem. Commun.*, 2008, 425–437; (*c*) R. L. Shook and A. S. Borovik, *Chem. Commun.*, 2008, 6095–6107; (*d*) N. S. Sickerman, Y. J. Park, G. K.-Y. Ng, J. E. Bates, M. Hilkert, J. W. Ziller, F. Furche and A. S. Borovik, *Dalton Trans.*, 2012, **41**, 4358–4364; (*e*) D. C. Lacy, J. Mukherjee, R. L. Lucas, V. W. Day and A. S. Borovik, *Polyhedron*, 2013, **52**, 261–267; (*f*) M. Adelhardt, M. J. Chalkley, F. W. Heinemann, J. Sutter, A. Scheurer and K. Meyer, *Inorg. Chem.*, 2014, **53**, 2763–2765; (*g*) E. M. Matson, J. A. Bertke and A. R. Fout, *Inorg. Chem.*, 2014, **53**, 4450–4458.

6 (*a*) K. J. Blackmore, J. W. Ziller and A. F. Heyduk, *Inorg. Chem.*, 2005, **44**, 5559–5561; (*b*) K. J. Blackmore, M. B. Sly, M. R. Haneline, J. W. Ziller and A. F. Heyduk, *Inorg. Chem.*, 2008, **47**, 10522–10532.

7 M. R. Haneline and A. F. Heyduk, *J. Am. Chem. Soc.*, 2006, **128**, 8410–8411.

8 J. A. Kopec, S. Shekar and S. N. Brown, *Inorg. Chem.*, 2012, **51**, 1239–1250.

9 C.-M. Liu, E. Nordlander, D. Schmeh, R. Shoemaker and C. G. Pierpont, *Inorg. Chem.*, 2004, **43**, 2114–2124.

10 T. Marshall-Roth, S. C. Liebscher, K. Rickert, N. J. Seewald, A. G. Oliver and S. N. Brown, *Chem. Commun.*, 2012, **48**, 7826–7828.

11 S. Shekar and S. N. Brown, *Dalton Trans.*, 2014, **43**, 3601–3611.

12 M. M. Hänninen, P. Paturi, H. M. Tuononen, R. Sillanpää and A. Lehtonen, *Inorg. Chem.*, 2013, **52**, 5714–5721.

13 X. Wu, M. A. Dube and A. J. Fry, *Tetrahedron Lett.*, 2006, **47**, 7667–7669.

14 N. G. Connelly and W. E. Geiger, *Chem. Rev.*, 1996, **96**, 877–910.

15 M. J. Frisch, G. W. Trucks, H. B. Schlegel, G. E. Scuseria, M. A. Robb, J. R. Cheeseman, G. Scalmani, V. Barone, B. Mennucci, G. A. Petersson, H. Nakatsuji, M. Caricato, X. Li, H. P. Hratchian, A. F. Izmaylov, J. Bloino, G. Zheng, J. L. Sonnenberg, M. Hada, M. Ehara, K. Toyota, R. Fukuda, J. Hasegawa, M. Ishida, T. Nakajima, Y. Honda, O. Kitao, H. Nakai, T. Vreven, J. A. Montgomery Jr., J. E. Peralta, F. Ogliaro, M. Bearpark, J. J. Heyd, E. Brothers, K. N. Kudin, V. N. Staroverov, R. Kobayashi, J. Normand, K. Raghavachari, A. Rendell, J. C. Burant, S. S. Iyengar, J. Tomasi, M. Cossi, N. Rega, J. M. Millam, M. Klene, J. E. Knox, J. B. Cross, V. Bakken, C. Adamo, J. Jaramillo, R. Gomperts, R. E. Stratmann, O. Yazyev, A. J. Austin, R. Cammi, C. Pomelli, J. W. Ochterski, R. L. Martin, K. Morokuma, V. G. Zakrzewski, G. A. Voth, P. Salvador, J. J. Dannenberg, S. Dapprich, A. D. Daniels, O. Farkas, J. B. Foresman, J. V. Ortiz, J. Cioslowski and D. J. Fox, *Gaussian 09, Revision A.02*, Gaussian, Inc., Wallingford CT, 2009.

16 G. M. Sheldrick, *Acta Crystallogr., Sect. A: Fundam. Crystallogr.*, 2008, **64**, 112–122.

17 *International Tables for Crystallography*, ed. A. J. C. Wilson, Kluwer Academic Publishers, Dordrecht, The Netherlands, 1992, vol. C.

18 P. Chaudhuri, M. Hess, J. Müller, K. Hildenbrand, E. Bill, T. Weyhermüller and K. Wieghardt, *J. Am. Chem. Soc.*, 1999, **121**, 9599–9610.

19 P. N. O'Shaughnessy, P. D. Knight, C. Morton, K. M. Gillespie and P. Scott, *Chem. Commun.*, 2003, 1770–1771.

20 C. Mukherjee, T. Weyhermüller, E. Bothe and P. Chaudhuri, *Inorg. Chem.*, 2008, **47**, 11620–11632.

21 K. S. Min, T. Weyhermüller, E. Bothe and K. Wieghardt, *Inorg. Chem.*, 2004, **43**, 2922–2931.

22 (*a*) C. N. Verani, S. Gallert, E. Bill, T. Weyhermüller, K. Wieghardt and P. Chaudhuri, *Chem. Commun.*, 1999, 1747–1748; (*b*) H. Chun, C. N. Verani, P. Chaudhuri, E. Bothe, E. Bill, T. Weyhermüller and K. Wieghardt, *Inorg. Chem.*, 2001, **40**, 4157–4166; (*c*) S. Mukherjee, T. Weyhermüller, E. Bothe, K. Wieghardt and P. Chaudhuri, *Dalton Trans.*, 2004, 3842–3853; (*d*) S. Mukherjee, T. Weyhermüller, E. Bill, K. Wieghardt and P. Chaudhuri, *Inorg. Chem.*, 2005, **44**, 7099–7108; (*e*) P. Chaudhuri, R. Wagner, U. Pieper, B. Biswas and T. Weyhermüller, *Dalton Trans.*, 2008, 1286–1288; (*f*) D. Das, A. K. Das, B. Sarkar, T. K. Mondal, S. M. Mobin, J. Fiedler, S. Záliš, F. A. Urbanos, R. Jimenez-Aparicio, W. Kaim and G. K. Lahiri, *Inorg. Chem.*, 2009, **48**, 11853–11864; (*g*) M. N. Bochkarev, A. A. Fagin, N. O. Druzhkov, V. K. Cherkasov, M. A. Katkova, G. K. Fukin and Y. A. Kurskii, *J. Organomet. Chem.*, 2010, **695**, 2774–2780; (*h*) A. K. Das, R. Hübner, B. Sarkar, J. Fiedler, S. Záliš, G. K. Lahiri and W. Kaim, *Dalton Trans.*, 2012, **41**, 8913–8921.

23 J. H. Gorvin, *J. Chem. Soc., Perkin Trans. 1*, 1988, 1331–1335.

24 (*a*) M. B. Jones and C. E. MacBeth, *Inorg. Chem.*, 2007, **46**, 8117–8119; (*b*) R. Çelenligil-Çetin, P. Paraskevopoulou, R. Dinda, R. J. Staples, E. Sinn, N. P. Rath and P. Stavropoulos, *Inorg. Chem.*, 2008, **47**, 1165–1172; (*c*) P. Paraskevopoulou, L. Ai, Q. Wang, D. Pinnapareddy, R. Acharyya, R. Dinda, P. Das, R. Çelenligil-Çetin, G. Floros, Y. Sanakis, A. Choudhury, N. P. Rath and P. Stavropoulos, *Inorg. Chem.*, 2010, **49**, 108–122.

25 R. I. Walter, *J. Am. Chem. Soc.*, 1955, **77**, 5999–6002.

26 Y. He, H. Zhao, X. Pan and S. Wang, *Synth. Commun.*, 1989, **19**, 3047–3054.

27 (*a*) R. Sanz, Y. Fernández, M. P. Castroviejo, A. Pérez and F. J. Fañanás, *J. Org. Chem.*, 2006, **71**, 6291–6294; (*b*) A. M. Panagopoulos, M. Zeller and D. P. Becker, *J. Org. Chem.*, 2010, **75**, 7887–7892.

28 (*a*) K. Ley and F. Lober, *FRG Pat* No. 1 104 522, 1959; (*b*) L. A. Maslovskaya, D. K. Petrikevich, V. A. Timoshchuk and O. I. Shadyro, *Russ. J. Gen. Chem.*, 1996, **66**, 1842–1846; (*c*) P. Chaudhuri, C. N. Verani, E. Bill, E. Bothe, T. Weyhermüller and K. Wieghardt, *J. Am. Chem. Soc.*, 2001, **123**, 2213–2223; (*d*) O. I. Shadyro, V. L. Sorokin, G. A. Ksendova, G. I. Polozov, S. N. Nikolaeva, N. I. Pavlova, O. V. Savinova and E. I. Boreko, *Pharm. Chem. J.*, 2003, **37**, 399–401.

29 J. P. Wilshire, L. Leon, P. Bosserman and D. T. Sawyer, *J. Am. Chem. Soc.*, 1979, **101**, 3379–3381.
30 M. Quiroz-Guzman, A. G. Oliver, A. J. Loza and S. N. Brown, *Dalton Trans.*, 2011, **40**, 11458–11468.
31 S. Wanniarachchi, B. J. Liddle, B. Kizer, J. S. Hewage, S. V. Lindeman and J. R. Gardinier, *Inorg. Chem.*, 2012, **51**, 10572–10580.
32 A. H. Randolph, N. J. Seewald, K. Rickert and S. N. Brown, *Inorg. Chem.*, 2013, **52**, 12587–12598.
33 (*a*) D. J. Berg, S. J. Rettig and C. Orvig, *J. Am. Chem. Soc.*, 1991, **113**, 2528–2532; (*b*) M. Kanesato, T. Yokoyama, O. Itabashi, T. M. Suzuki and M. Shiro, *Bull. Chem. Soc. Jpn.*, 1996, **69**, 1297–1302; (*c*) C. Spino, L. L. Clouston and D. J. Berg, *Can. J. Chem.*, 1997, **75**, 1047–1054; (*d*) M. Kanesato and T. Yokoyama, *Chem. Lett.*, 1999, 137–138; (*e*) P. V. Bernhardt, B. M. Flanagan and M. J. Riley, *Aust. J. Chem.*, 2000, **53**, 229–231; (*f*) M. Kanesato and T. Yokoyama, *Anal. Sci.*, 2000, **16**, 335–336; (*g*) M. W. Essig, D. W. Keogh, B. L. Scott and J. G. Watkin, *Polyhedron*, 2001, **20**, 373–377; (*h*) M. Kanesato, F. N. Ngassapa and T. Yokoyama, *Anal. Sci.*, 2001, **17**, 473–474; (*i*) P. V. Bernhardt, B. M. Flanagan and M. J. Riley, *Aust. J. Chem.*, 2001, **54**, 229–232; (*j*) M. Kanesato, H. Houjou, Y. Nagawa and K. Hiratani, *Inorg. Chem. Commun.*, 2002, **5**, 984–988; (*k*) S. Mizukami, H. Houjou, M. Kanesato and K. Hiratani, *Chem. – Eur. J.*, 2003, **9**, 1521–1528; (*l*) W.-K. Wong, H. Liang, J. Guo, W.-Y. Wong, W.-K. Lo, K.-F. Li, K.-W. Cheah, Z. Zhou and W.-T. Wong, *Eur. J. Inorg. Chem.*, 2004, 829–836; (*m*) M. Kanesato, S. Mizukami, H. Houjou, H. Tokuhisa, E. Koyama and Y. Nagawa, *J. Alloys Compd.*, 2004, **374**, 307–310; (*n*) P. Dröse and J. Gottfriedsen, *Z. Anorg. Allg. Chem.*, 2008, **634**, 87–90; (*o*) P. Dröse, S. Blaurock, C. G. Hrib and F. T. Edelmann, *Z. Anorg. Allg. Chem.*, 2010, **636**, 1431–1434; (*p*) P. Dröse, C. G. Hrib and F. T. Edelmann, *Acta Crystallogr., Sect. E: Struct. Rep. Online*, 2010, **66**, m1386; (*q*) P. Dröse, J. Gottfriedsen, C. G. Hrib, P. G. Jones, L. Hilfert and F. T. Edelmann, *Z. Anorg. Allg. Chem.*, 2011, **637**, 369–373; (*r*) M. Kanesato, K. Nagahara, K. Igarashi, K. Sato, Y. Kikkawa and M. Goto, *Inorg. Chim. Acta*, 2011, **367**, 225–229.
34 (*a*) S. Liu, S. J. Rettig and C. Orvig, *Inorg. Chem.*, 1992, **31**, 5400–5407; (*b*) P. K. Bharadwaj, A. M. Lee, S. Mandal, B. W. Skelton and A. H. White, *Aust. J. Chem.*, 1994, **47**, 1799–1803; (*c*) J. Parr, A. T. Ross and A. M. Z. Slawin, *Main Group Chem.*, 1998, **2**, 243–249; (*d*) X.-X. Zhou, Y.-P. Cai, S.-Z. Zhu, Q.-G. Zhan, M.-S. Liu, Z.-Y. Zhou and L. Chen, *Cryst. Growth Des.*, 2008, **8**, 2076–2079; (*e*) D. M. J. Doble, A. J. Blake, D. E. Hibbs, M. S. Jackson, W.-S. Li and M. Schröder, *Z. Anorg. Allg. Chem.*, 2002, **628**, 2311–2314.
35 (*a*) D. M. J. Doble, A. J. Blake, W.-S. Li and M. Schröder, *J. Chem. Soc., Dalton Trans.*, 2001, 3137–3139; (*b*) T. Shiga and H. Oshio, *Polyhedron*, 2007, **26**, 1881–1884.
36 (*a*) C. G. Pierpont and R. M. Buchanan, *Coord. Chem. Rev.*, 1981, **38**, 45–87; (*b*) C. G. Pierpont and C. W. Lange, *Prog. Inorg. Chem.*, 1994, **41**, 331–442; (*c*) B. de Bruin, E. Bill, E. Bothe, T. Weyhermüller and K. Wieghardt, *Inorg. Chem.*, 2000, **39**, 2936–2947; (*d*) H. Chun, P. Chaudhuri, T. Weyhermüller and K. Wieghardt, *Inorg. Chem.*, 2002, **41**, 790–795; (*e*) S. Bhattacharya, P. Gupta, F. Basuli and C. G. Pierpont, *Inorg. Chem.*, 2002, **41**, 5810–5816.
37 S. N. Brown, *Inorg. Chem.*, 2012, **51**, 1251–1260.
38 N. Deibel, D. Schweinfurth, S. Hohloch, M. Delor, I. V. Sazanovich, M. Towrie, J. A. Weinstein and B. Sarkar, *Inorg. Chem.*, 2014, **53**, 1021–1031.
39 S. Amthor, B. Noller and C. Lambert, *Chem. Phys.*, 2005, **316**, 141–152.
40 E. J. Palmer and B. E. Bursten, *Polyhedron*, 2006, **25**, 575–584.
41 (*a*) D. P. Tate, J. M. Augl, W. M. Ritchey, B. L. Ross and J. G. Grasselli, *J. Am. Chem. Soc.*, 1964, **86**, 3261–3265; (*b*) R. B. King, *Inorg. Chem.*, 1968, **7**, 1044–1046.
42 D. L. Morrison, P. M. Rodgers, Y.-W. Chao, M. A. Bruck, C. Grittini, T. L. Tajima, S. J. Alexander, A. L. Rheingold and D. E. Wigley, *Organometallics*, 1995, **14**, 2435–2446.
43 T. B. Karpishin, M. S. Gebhard, E. I. Solomon and K. N. Raymond, *J. Am. Chem. Soc.*, 1991, **113**, 2977–2984.
44 T. B. Karpishin, T. M. Dewey and K. N. Raymond, *J. Am. Chem. Soc.*, 1993, **115**, 1842–1851.
45 M. Lein, A. Szabó, A. Kovács and G. Frenking, *Faraday Discuss.*, 2003, **124**, 365–378.
46 Ò. González-Blanco, V. Branchadell, K. Monteyne and T. Ziegler, *Inorg. Chem.*, 1998, **37**, 1744–1748.
47 If the reference state of the ligating atom contains singly occupied pπ levels, much greater π bonding energies are obtained due to the strongly favorable electron transfer from metal to ligand. See, *e.g.*, K. K. Pandey and G. Frenking, *Eur. J. Inorg. Chem.*, 2004, 4388–4395.

Undergraduate Research Symposium – May 1, 2015

Slatt Scholar: Andrew Neils
Department of Chemical and Biomolecular Engineering

Advisor: Dr. Prashant Kamat, Department of Chemistry and Biochemistry, Department of Chemical and Biomolecular Engineering, Radiation Laboratory

Understanding Metal-Semiconductor Interactions in Core-Shell=Shell Au-SiO2-Cds Particle

During the 2014-2015 school year, an understanding of the role and the effect of methanol in the electrolyte of quantum dot solar cells (QDSCs) was explored. Previous researchers have claimed that use of a traditional polysulfide electrolyte spiked with methanol promotes higher efficiencies. Once an electron is excited in a QDSC, methanol or other compounds can regenerate the charge lost in the quantum dot by donating an electron to the valence band of the semiconductor particle. This process requires a continuous flow of charges to maintain the photovoltaic output and stability of the QDSC. However the issue with methanol is that upon donation of an electron it irreversibly decomposes and in the process can contribute additional electrons as a result of chemical reactions and not light absorption, therefore artificially enhancing the QDSC in an unsustainable way. As described, this leads to the gradual consumption of methanol molecules, which is why the compound is called a sacrificial donor. The experiments performed throughout the last year sought to reveal the true role of methanol in the QDSC operation.

Our initial studies involved probing the electron transfer reaction between methanol and CdSe quantum dots. The rate of these reactions was compared to the standard regenerative processes that occur when using prototypical polysulfide electrolyte (S^{2-}/S_n^{2-}). Using steady state and time resolved photoluminescence spectroscopy, we were able to quantify the rate and degree of electron transfer in these different electrolyte solutions. The competition kinetics in regenerating quantum dot charges shed light on methanol's activity in the electrolyte solution. Following this work, QDSCs were made with and without methanol in the electrolyte to study the effects on efficiency and longevity of the cell. The results indicate minor, if any, benefits from using methanol in the electrolyte. Additionally, long-term tests on the QDSCs showed that with larger amounts of methanol in the electrolyte, the current decreased more rapidly than with an aqueous polysulfide electrolyte.

Oral Presentation

Providing Better Tools for Responsible Design

Francis Rogg
Advisor: Aimee Buccellato, School of Architecture, University of Notre Dame

Because about 40% of America's energy is consumed in building operations, great care must be taken by architects and engineers to design in an informed and responsible manner. The vast majority of design is now undertaken with the aid of computers and so it is imperative that architects and engineers be armed with competent software tools for analyzing the potential environmental impact of proposed buildings. Unfortunately, the reality of the situation is that tools of this nature available today are quite rudimentary. A quality energy analysis tool should include several key features, and all currently available tools are missing at least one of the following critical attributes; the tool should be reliably accurate and precise, should react dynamically and be usable during the design process, should make a holistic assessment of impact, and last but not least, it should be user-friendly. Here at the Green Scale Project our own new tool is in its testing phases, but in parallel with tool development time has been devoted to the analysis of case studies using several of the most popular environmental impact tools available. This comparative study is revealing the strengths and weaknesses of these commonplace tools and shows examples of the numerical variance between each of their respective outputs under a controlled experimental situation. Both the discrepancies discovered between these existing applications and the inherent weaknesses identified in this study support the need for a new tool. The particular attributes being written into the code of the Green Scale Tool respond to the shortcomings found in existing applications and should give designers a chance to practice in a more conscientious manner with far more confidence and far less effort. Providing this capability to architects everywhere has the potential to fundamentally shift the industry towards adopting more sustainable practices as habit, thereby paring down what is now an enormous sector of the planet's energy consumption. In this way, humanity can become better, more caring stewards of what is now its only home.

Anna Sliwinski, Department of Chemistry (Slatt Scholar)
Dr. Haifeng Gao, Department of Chemistry (Faculty Advisor)

Quantification of Side Reactions in SCVcP of A-BIEM and MMA Hyperbranched Polymer

Hyperbranched polymers have many useful properties, including low viscosity and high solubility, that translate well to development in the coatings industry, drug delivery, and nanotechnology.[1,2] Traditionally, hyperbranched polymers can be synthesized with a facile one-pot self-condensing vinyl co-polymerization (SCVcP), a sharp contrast to the multi-step synthesis of dendrimers, the structural analogs of hyperbranched polymers. However, the hyperbranched polymers synthesized in the one-pot reaction suffer from poorly defined structure, high polydispersities, and are difficult to characterize due to inevitable side reactions. Therefore, quantifying these side reactions can make polymer characterization easier and improve the utility of hyperbranched polymerization. In this project, 2-(1-(2-((2-bromo-2-methylpropanoyl)oxy) ethoxy)ethoxy)ethyl methacrylate (A-BIEM) inimer and methyl methacrylate (MMA) were copolymerized to synthesize a degradable hyperbranched polymer. The reaction kinetics were monitored with samples being taken at intervals of about 25%, 50%, 75%, 99% conversion. The samples were then degraded and the fragments were analyzed by size exclusion chromatography to identify and quantify the side reactions, more specifically radical-radical coupling, occurring in the reaction with increased conversion.

[1]Segawa, Y.; Higashihara, T.; Ueda, M. *Polym. Chem.* **2013**, *4*, 1746-1759.
[2] Gao, C.; Yan, D. Hyperbranched Polymers: from synthesis to applications. *Prog. Polym. Sci.* **2004,** *29,* 183-275.

Developing a Practical Characterization Tool to Investigate the Structure of Hyperbranched Polymers

Anna Sliwinski, Xiaofeng Wang, Robert Graff, and Haifeng Gao
Department of Chemistry & Biochemistry, University of Notre Dame, Notre Dame, IN 46556

INTRODUCTION:

Hyperbranched polymers (HBP) have many useful properties that include low viscosity and high solubility, and could find promising applications in the fields of drug delivery, coatings and additive development, as well as the development of lubricants, additives. Traditionally, hyperbranched polymers are synthesized with a facile one-pot self-condensing vinyl co-polymerization (SCVcP), a sharp contrast to the multi-step synthesis of dendrimers, which are structural analogs of hyperbranched polymers (figure 1). However, hyperbranched polymers synthesized in the one-pot reaction suffer from poorly defined structure, high polydispersities, and are difficult to characterize due to various side reactions. Quantifying these side reactions can make polymer characterization easier and improve the utility of hyperbranched polymerization. This project was focused on designing a method to characterize the HBP and identify radical termination reactions occurring in the SCVcP of 2-(1-(2-((2-bromo-2-methylpropanoyl)oxy)ethoxy)ethoxy)ethyl methacrylate (A-BIEM) inimer and methyl methacrylate (MMA) monomer to synthesize a degradable hyperbranched polymer. The reaction kinetics were monitored at intervals of about 25%, 50%, 75%, 99% conversion. They were then degraded and the fragments were analyzed by size exclusion chromatography (SEC) to help gain a better understanding of how the molecular weight distribution changed before and after degradation. The goal was then to confirm the presence of coupling peaks by developing a standard for comparison.

METHOD DEVELOPMENT:

1. **Choosing a degradable inimer to allow for analysis after polymerization**

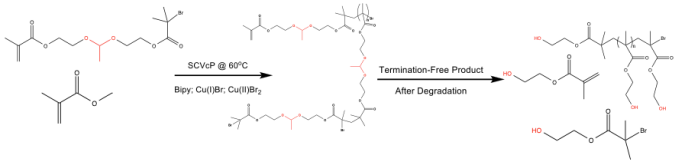

Figure 1. Reaction Scheme for HBP synthesis and degradation. HB are difficult to characterize after polymerization due to their exceptionall large masses. Including a degradable polymer in the reaction desig allowed us to selectively cleave the resulting polymer into smalle polymers that could be analyzed by SEC. The expected results from reaction with no termination are shown at the far right.

2. **Identifying expected termination reactions**

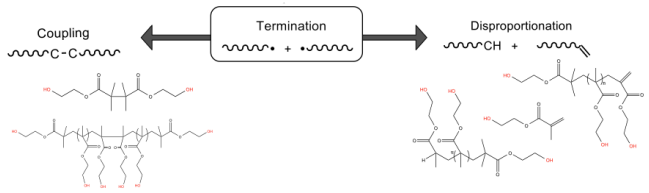

Figure 2. Resultant Products due to one of two types of terminatic coupling or disproportionation. Termination is the reaction of two acti radicals in the solution. This essentially stops the reaction, so the mo termination that occurs the slower and less productive the reaction becom Understanding the expected termination reactions reveals a property of the polymer products that differs from the non-termination product: they a likely to be twice the molecular weight on average, as they are two sing polymers combined. Therefore, we can identify these products in SI separately from the non-termination single chain product.

3. **Synthesizing HBP, Analyzing in SEC and Identifying Peaks**

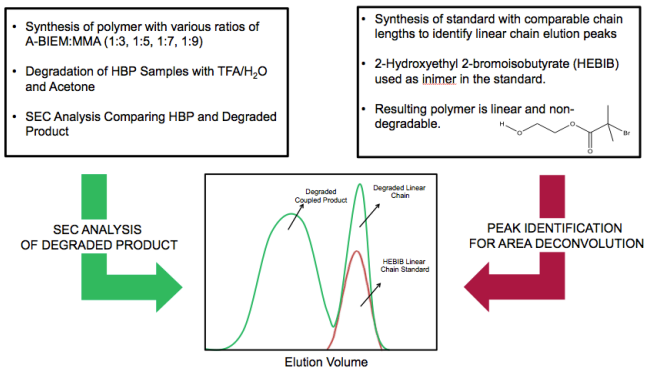

Figure 3. Two Pronged Approach to Analyzing and Identifying Sing Chain and Coupling Peaks in SEC. While synthesizing various polym samples (green) a single chain standard was also synthesized (red) to compa for proper peak selection. This standard had the same chain length as t expected single chain lengths of a given inimer/monomer ratio.

RESULTS:

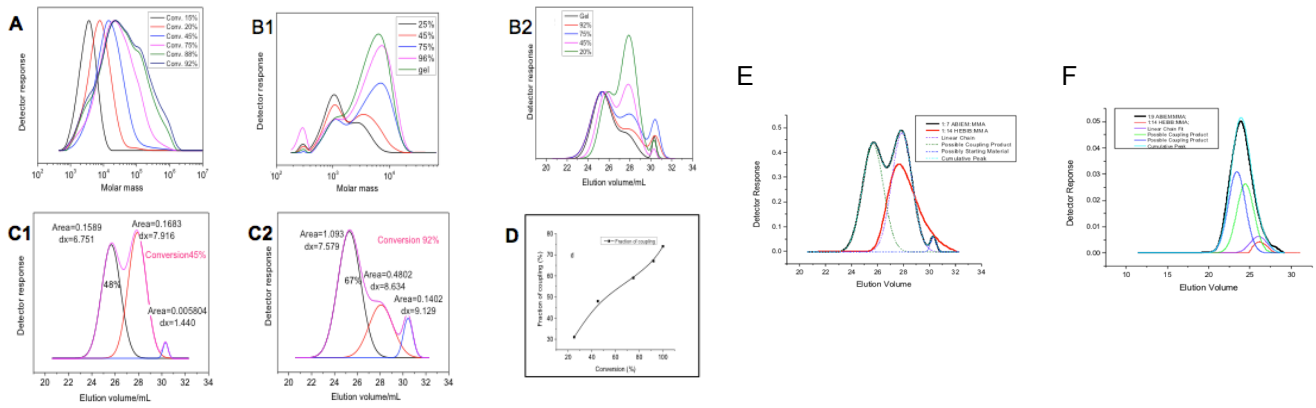

Figure 4. SEC Results. (A-D 1:7 ABIEM:MMA) & (E 1:7 ; F 1:9). A) HBP molar mass evolution with increasing conversion. B1) Degraded product (molar mass). B2) Degaded product (elution volume). C1) Deconv. of 48% conv. sample. C2) Deconv. of 92% conv. sample. D) % Coupling as function of conversion. *Syntheses of 1:3; 1:5; 1:9 had similar results of increased coupling with increased conversion.* E) The 48%1:14 HEBIB:MMA standard (red) matches expected single chain peak in well-defined peak separation of 1:7 ABIEM:MMA at 18% conv. F) The 28%1:14 HEBIB:MMA standard (red) matches expected single chain peak in poorly-defined peak separation of 1:9 ABIEM:MMA at 46% conv.

DISCUSION AND CONCLUSIONS:

This project resulted in the development of a practical experimental design to characterize the structure of HBP. The current method shows the utility the degradable inimer initiator as well as the benefit of synthesizing a linear standard for comparison. However, it is necessary to fine-tune the standard synthesis so that it can better reflect and represent nuances in the possible degraded products (figure 5). A lot of work was done improving the purification procedure after degradation to remove the water without disrupting the polymer composition. Two different methods (extraction and simple evaporation) were used. Both were successful (Figure 4 E is a result of extraction Figure 4 F is a results of evaporation method). The evaporation method has shown wider, less distinct peak separation. There are many factors that could bring about this result. For one the evaporation method could be more effective at avoiding fractionation (selective purification of larger polymers) and therefore retains polymer fractions that are removed by the extraction purification. Additionally, this could be the result of incomplete degradation. Degradation is checked by observing the disappearance of the acetal hydrogen (4.9 ppm) in NMR. When I took over the project in my second semester, at some points degradation was confirmed by judging the opacity of the solutions as well as the amount of time that the solutions had been degrading due to schedule constraints (if the solution changes from cloudy to clear then the particles in solution have become smaller, ie been degraded). In the future, the NMR should be done for all samples routinely (even within the same batch being degraded every sample should be treated individually). A third addition to the experimental design would be to do a chain extension, where the resultant, degraded polymers are reacted once more with MMA (1:50 respectively). This reaction would result in live chains growing by an average of 50 MMA units while dead chains will be inactive. By running SEC analysis after the reaction it will be possible to quantify the ratio of dead to living chains after a particular conversion of the initial HBP polymerization.

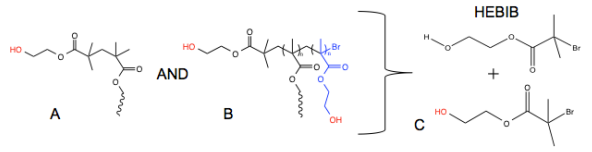

Figure 5. Improvement of standard design. Structures A and B are possible products for the non-termination pathway. B has an extra possible addition (blue). Preparing the standard linear chain with 1:X:1 HEBIB:MMA:Monomer C accounts for this extra addition of molecular weight that could be affecting how well the standard represents the degraded linear A-BIEM based polymer.

References:

[1] Segawa, Y.; Higashihara, T.; Ueda, M. *Polym. Chem.* **2013**, *4*, 1746-1759.
[2] Gao, C.; Yan, D. Hyperbranched Polymers: from synthesis to applications. *Prog. Polym. Sci.* **2004,***29,* 183-275.
[3] Higashihara, T.; Segawa, Y; Sinananwanich, W.; Ueda, M. *Polym. J.* **2012**, *44*, 14-29.

Acknowledgements:
Vincent P. Slatt Fellowship for Undergraduate Research in Energy Systems and Processes.
ND Energy: Center for Sustainable Energy at Notre Dame

Cerium Incorporated ZSM-5 & ZSM-12's for the Conversion of Biomass Model Compounds to Chemicals

Kwan Lai Leon Tong
Major: Chemical Engineering
Advisor: Jason C. Hicks, Dept. of Chemical & Biomolecular Engineering, University of Notre Dame

Fossil fuels are widely used in the energy sector especially for transportation and the generation of electricity. However, reliance on fossil fuels leads to several consequences including CO_2 emission, which would cause environmental damages. To solve this problem, scientists and engineers have been trying to find renewable energy sources. One of the renewable energy sources is biofuels derived from biomass. First generation biofuel is derived from corn. A good example is ethanol. An alternative feedstock is lignocellulosic biomass, which is composed of cellulose, hemicellulose and lignin. Zeolites can be used as catalysts to convert these diverse feedstocks into fuels and chemicals by increasing the yield and selectivity to aromatic products. They can easily be integrated into existing petroleum refineries and are versatile for different types of lignocellulosic biomass feedstocks.[1] My research focuses on the performance of cerium incorporated ZSM-12 and ZSM-5. Both zeolites have different frameworks, pore structures and pore sizes. The main chemical property that enables zeolites to improve the selectivity of the aromatic products upgrade is their catalytic acid sites. Using catalytic fast pyrolysis, biomass feedstocks can be effectively converted into desired aromatic products under rapid heating to temperature between 400 to 700 ^{o}C in the absence of oxygen. The products are subsequently analyzed using gas chromatography and mass spectroscopy. The results show that the four different catalysts (ZSM-5, Ce-ZSM-5, ZSM-12, Ce-ZSM-12) all have a different yield and selectivity with respect to the biomass feedstock.

What inspired you to participate in undergraduate research?

The study of catalysis has always been my interest since I completed my high school Chemistry thesis on Monophenolase on the browning process of apples. Coincidentally, Professor Hicks' group also focuses on catalysis and its application on renewable energy like biofuel.

How did you get your research position, and what preparation did you undertake for it?

I contacted Professor Hicks through email and he agreed to meet up with me to discuss about his research group and the potential project I would be undertaking. He also recommended me to apply for the 2014 Slatt Fellowship for funding for my research and stipend during the summer

Where was your research experience located?

"University of Notre Dame"

What did you get out of your research experience?

I was exposed to different analytical chemistry techniques and specialized organic chemistry theories that are pertinent to biofuels. Those are the knowledge that is not covered in classes. I also got to know the graduate students in the group better and Professor Hicks through weekly group lunch. The most rewarding part is that it allows me to see whether graduate school would be a fit for me in the future.

(1) Hicks, Jason C. "Advances in C–O Bond Transformations in Lignin-Derived Compounds for Biofuels Production." *The Journal of Physical Chemistry Letters*(2011): 2280-282. Web.

Undergraduate Summer Research at University of Notre Dame

Name: Thelmar Manyika

Advisor: Philip Smith

Project:

Slow evaporation and Ionothermal reactions

Objective:

To gain a better insight into the relationships between topologies of the structural units and the interstitial complexes in uranyl compounds at relatively low temperature via slow evaporation in aqueous media, or in the absence of excess water by ionothermal reactions.

Nature:

We carried out experiments investigating the ionothermal effects on the synthesis of uranyl coordination compounds. We prepared approximately 60reactions. Constituents were typically reacted in integral molar ratios with the uranyl salts. Some of the reactions were reacted with ionic liquid BMIM Dy(NCS)6, a few of them used AcyIL instead and a lot of the later reactions did not use ionic liquids.

In some of the reactions a precipitate was formed upon the addition of a reactant to a reaction vial. In such situations a solvent was added to dissolve the precipitate if possible for example hydrochloric acid was used as a solvent. In some cases water and MeCN were added to our reactions to aid dissolution in case of AS2O5 it was left in water for a few hours until it dissolved. Some of the reactions were thermal reactions so they were put in bombs and placed in an oven either at 120 degrees for five days or 140 degrees for seven days. This was simply because some of their reactions require high temperatures to occur. The rest of the samples were left to react under ambient conditions.

Results:

We later analyzed all of our results and some of the reactions yielded crystalline products. We could easily tell just by looking that no crystal had been formed from all the reactions that did not produce any precipitate. We then carried out vacuum filtration on the remaining samples. We then analyzed what we had recovered from the filtration on a microscope.

Under the microscope we were able to select a single crystal from each sample. We used these single crystals to determine the structural composition of the crystals yielded by our reactions by carrying out

an x-ray diffraction experiment. The crystals were mounted on a cryoloop and the experiment was left overnight while data regarding the crystal was being collected. We then used the Apex 2 software from the desktop to refine the unit-cell parameters and collect all the information which was later used to derive the formula for the crystal.

Crystals formed:

During our research we had the opportunity to observe many crystals that had been formed from our reactions. Below are some of the crystallographic data and refinement parameters for some of the crystals yielded by our reaction.

Formula	PAS 253	PAS 215	PAS 220
Bond precision	C-C = 0.0060 A	C-C = 0.0143 A	C-C = 0.0135 A
Wavelength	0.71073	0.71073	0.71073
a (A)	8.1660(15)	7.4042(11)	8.5103(7)
b (A)	8.1660(15)	13.468(2)	12.1693(11)
c (A)	10.752(2)	29.066(4)	13.4350(12)
alpha	90	94.1880(19)	99.977(1)
Beta	90	92.580(2)	104.554(1)
Gamma	90	96.490(2)	100.504(1)
Temperature	296K	140K	183K
Volume	717.0(3)	2868.0(7)	1288.6(2)
Space group	P 41 21 2	P -1	P-1
Hall group	P 4abw 2nw	-P 1 :C5 N5 O2 S5 U, 2(C15 H9	P-1
Moiety formula	C4 O7 U	N3), C15 H7 N3, H N O2, C,2(Na)	C24 Cl2 N8 O12 U2, 2(C2 F6N O4 S2)
Sum formula	C4 O7 U	C51 H26 N15 Na2 O4 S5 U	C28 Cl2 F12 N10 O20 S4 U2
Mr	398.07	1357.18	1699.58
Dx,g cm-3	3.688	1.572	2.190
Z	4	2	1
Mu (mm-1)	22.635	3.084	6.664
F000	688.0	1326.0	788.0
F000’	650.65	1308.47	770.13
h,k,lmax	10,10,14	9,17,37	11,15,17
Nref	837[532]	13332	6039

A) 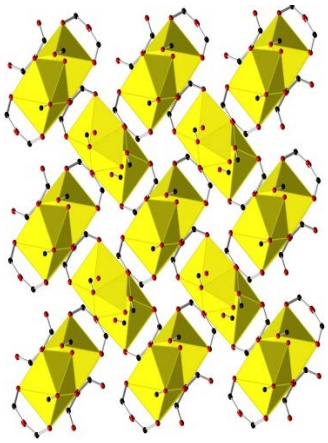

B) 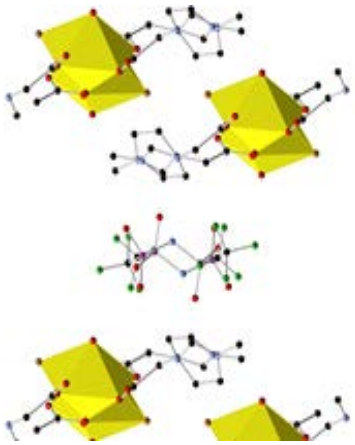

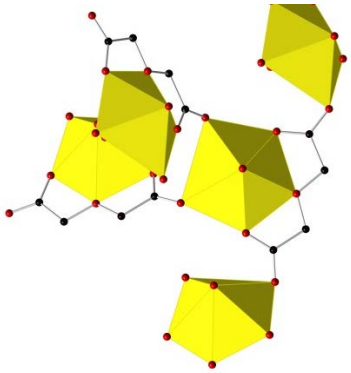

A)

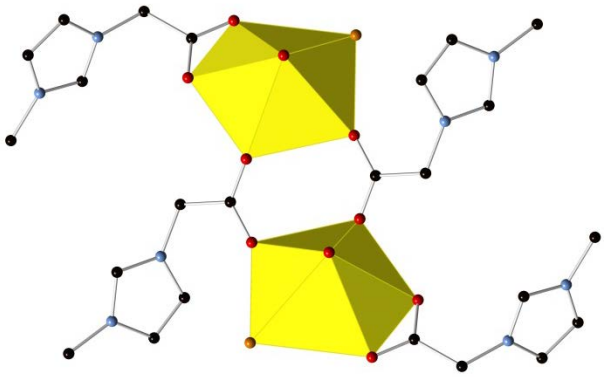

B)

A are some of the images which are showing PAS 253 while B is representing images showing PAS 220. The two crystals are not the same as represented by the images. The top B image shows that there was another element present in the uranium crystal other than the crystal itself. The bottom images show that there were more uranium atoms in A than in B.

Conclusion

I had an opportunity to learn a lot about uranium crystals. I learned about how crystals form, the filtration process and how to determine the structure of the crystals using the x-ray diffractometer.